Na_2CO_3. Since $CO_2\cdot^-$ can convert to $O_2\cdot^-$ and $HO_2\cdot$ in the presence of oxygen, the oxidation of hydrogen peroxide (H_2O_2) was tested to compare with that of formate. In the peroxide-persulfate reaction, the reaction rates between pH 0.7 and 5 were almost constant, in contrast with the pH dependence in the formate-persulfate reaction. On the other hand, the reaction rate decreases greatly in an alkaline solution. This fact may indicate that $O_2\cdot^-$ is much less reactive than $HO_2\cdot$. In order to account for the characteristics of the pH dependence, the order in reactivity of radicals in the formate-persulfate reaction may be postulated to be as $HCO_2H\cdot^+ < HCO_2\cdot < CO_2\cdot^- > O_2CO_2\cdot^- > HO_2\cdot > O_2\cdot^-$. In case of a chain reaction involving several radicals, there are generally more factors to affect the rate of reaction. Since many reactions in the separate steps are competing against each other, the rate in each step and the lifetime of the radicals are also important factors to determine the overall reaction rate. The inhibiting effect of iron(III) is briefly accounted for by the following reactions.

$$Fe(III) + CO_2\cdot^- \rightarrow Fe(II) + CO_2 \quad (17)$$

$$Fe(II) + SO_4\cdot^- \rightarrow Fe(III) + SO_4^{2-} \quad (18)$$

Considering that the inhibiting effect of iron was not large, the above chain reaction does not seem to be fast under the conditions. Some iron ions may hydrolyze; in fact, the reaction mixture was slightly turbid at 2×10^{-4} *M* Fe(III) in Table VI. Under the same conditions, copper(II) was a very powerful catalyst. The copper catalysis will be accounted for by reactions 19 and 20.

$$Cu(II) + CO_2\cdot^- \rightarrow Cu(I) + CO_2 \quad \text{(fast)} \quad (19)$$

$$S_2O_8^{2-} + Cu(I) \rightarrow Cu(II) + SO_4\cdot^- + SO_4^{2-} \quad \text{(fast)} \quad (20)$$

Acknowledgment. The financial support of a research grant from the Japanese Ministry of Education for this project is gratefully acknowledged.

Appendix

The following reactions for the radical species are predicted according to the pH change. In the absence of oxygen

$$HCOOH\cdot^+ \rightleftarrows HCOO\cdot + H^+ \quad (21)^{8}$$

$$HCOO\cdot \rightleftarrows CO_2\cdot^- + H^+ \quad pK_a = 3.9 \quad (22)^{15}$$

$$CO_3^{2-} + OH\cdot \rightarrow CO_3\cdot^- + OH^- \quad k = 4.2 \times 10^8\ M^{-1}\ sec^{-1} \quad (23)^{16}$$

$$CO_3^{2-} + SO_4\cdot^- \rightarrow CO_3\cdot^- + SO_4^{2-} \quad (24)$$

$$HCO_3^- + OH\cdot \rightarrow CO_3\cdot^- + H_2O \quad k = 1.5 \times 10^7\ M^{-1}\ sec^{-1} \quad (25)^{16}$$

$$HCO_3\cdot \rightleftarrows CO_3\cdot^- + H^+ \quad pK_a = 9.6 \quad (26)^{17}$$

$$OH\cdot \rightleftarrows O\cdot^- + H^+ \quad pK_a = 10.9 \quad (27)^{16,18,19}$$

In the presence of oxygen

$$CO_2\cdot^- + O_2 \rightleftarrows O_2CO_2\cdot^- \quad K = 4 \times 10^5\ M^{-1} \quad (28)^{1}$$

$$CO_2\cdot^- + O_2 \rightarrow CO_2 + O_2\cdot^- \quad (29)^{15}$$

$$CO_2\cdot^- + O_2 + H^+ \rightarrow HO_2\cdot + CO_2 \quad (30)^{2,15,18,20}$$

$$HO_2\cdot + H^+ \rightleftarrows H_2O_2\cdot^+ \quad (31)$$

$$HO_2\cdot \rightleftarrows H^+ + O_2\cdot^- \quad pK_a = 4.8 \quad (32)^{20,21}$$

Registry No. $HCOO^-$, 71-47-6; $S_2O_8^{2-}$, 15092-81-6.

(15) A. Fojtik, G. Czapski, and A. Henglein, *J. Phys. Chem.*, 74, 3204 (1970).
(16) J. L. Weeks and J. Rabani, *J. Phys. Chem.*, 70, 2100 (1966).
(17) S. Chen, V. W. Cope, and M. Z. Hoffman, *J. Phys. Chem.*, 77, 1111 (1973).
(18) G. V. Buxton, *Trans. Faraday Soc.*, 65, 2150 (1970).
(19) J. Rabani and M. S. Matheson, *J. Phys. Chem.*, 70, 761 (1966).
(20) D. Behar, G. Czapski, L. M. Dorfman, J. Rabani, and H. A. Schwarz, *J. Phys. Chem.*, 74, 3209 (1970).
(21) J. Rabani and S. O. Nielsen, *J. Phys. Chem.*, 73, 3736 (1969).

Contribution from the Department of Chemistry, University of Victoria, Victoria, British Columbia, Canada

Nuclear Magnetic Resonance Spectra of Platinum(II) Hydrides. AB_2X and AB_2MX Spin Systems

THOMAS W. DINGLE and KEITH R. DIXON*

Received September 10, 1973

^1H and ^{31}P nuclear magnetic resonance spectra are reported for the complex cations $[PtH(PEt_3)_3]^+$, *trans*-$[PtH(PEt_3)_2(PPh_3)]^+$, and $[PtH(PPh_3)_3]^+$. The hydridic hydrogen resonances of these cations show different center-band and ^{195}Pt side-band multiplet structures. An approximate analysis using the AB_2X and AB_2MX spin systems (A = B = ^{31}P, M = ^{195}Pt, and X = ^1H) clearly shows the reasons for these differences and demonstrates that similar side- and center-band spectra occur only if $|\delta_{AB}| \gg {}^1/_2|J_{AM} - J_{BM}|$. Similar results are expected for related spin systems of the $A_nB_m(M)X$ type. In certain circumstances (when $|\delta_{AB}| \simeq {}^1/_2|J_{AX} - J_{BX}| - |J_{AB}||$ in our particular cases) this type of analysis is not valid and it may be necessary to include the effects of remote magnetically active nuclei such as the protons in the tertiary phosphine ligands.

Introduction

Roundhill and coworkers[1] have recently described an example of a platinum complex, $[PtH(PPh_3)_3][(CF_3COO)_2H]$, in which the nuclear magnetic resonance (nmr) spectrum of the hydridic hydrogen shows different multiplet structures in the side bands (due to molecules containing ^{195}Pt, 33.8% abundant, $I = {}^1/_2$) and in the center band (due to molecules containing other platinum isotopes). These workers discussed their results using computer-simulated spectra for the AB_2X and AB_2MX spin systems but were unable to find a set of coupling parameters which would explain both side- and

(1) K. Thomas, J. T. Dumler, B. W. Renoe, C. J. Nyman, and D. M. Roundhill, *Inorg. Chem.*, 11, 1795 (1972).

center-band spectra. They also considered the possibility that ion association might cause chemical inequivalence of the mutually trans phosphorus atoms. We have recently encountered[2] similar problems in interpreting the ^{19}F nmr spectrum of $[PtF(PPh_3)_3][BF_4]$. Since platinum complexes are so widely studied and nmr spectra are frequently an important source of characterization data, it is of interest to investigate the circumstances under which these unusual spectra may be expected. In the present paper ^1H and ^{31}P nmr spectra are reported for several complexes of the $[PtH(PR_3)_3]^+$ type and an analysis, mainly in terms of the AB_2X and AB_2MX spin systems, clearly shows the reasons for the apparently anomalous spectra.

Results and Discussion

Theoretical Analysis. The complexes studied and the labeling of nuclei employed in the discussion are shown below

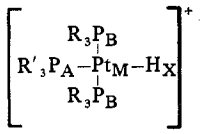

where R′ = R = ethyl or phenyl; R′ = phenyl, R = ethyl. The expected first-order splitting pattern for the X proton in molecules not containing ^{195}Pt is shown as the first line diagram in Figure 1. First-order coupling to ^{195}Pt in 33.8% of the molecules will produce high- and low-field side bands each having one-fourth of the intensity of the center band and each having a doublet of triplets structure identical with that of the center band. However, the previous study[1] of $[PtH(PPh_3)_3]^+$ at 100 MHz showed a quartet structure for the center band and triplets for the side bands and, as detailed below, we observe similar effects in our complexes.

The complete interpretation of these spectra is rather complex and is discussed in detail below. However, the basic features may be understood in terms of the AB_2X and AB_2MX spin systems, where the latter applies to molecules containing ^{195}Pt. The AB_2X system has been analyzed previously[3] and we have used standard procedures[4] to extend the analysis to the AB_2MX system. The results for transitions appearing in the X region of the spectrum are collected in Table I and inspection shows that each AB_2X line is related to two AB_2MX lines, one containing a $+^1/_2J_{MX}$ term and the other containing $-^1/_2J_{MX}$. All the expressions containing $+^1/_2J_{MX}$ are identical with the corresponding AB_2X expressions except that δ_{AB} (the chemical shift difference between the A and B phosphorus atoms) is replaced by $\delta_{AB} + {}^1/_2(J_{AM} - J_{BM})$. Similarly the expressions containing $-^1/_2J_{MX}$ have $\delta_{AB} - {}^1/_2(J_{AM} - J_{BM})$. Thus the AB_2MX system in the X region may be analyzed as two AB_2X subspectra having the general appearance expected for AB_2X spectra with effective chemical shifts, $\delta_{AB}^{eff} = \delta_{AB} \pm {}^1/_2(J_{AM} - J_{BM})$, and separated by J_{MX}. This analysis is, of course, similar to the concept of effective Larmor frequencies which is often used in simpler systems. In our case J_{MX} is large and the subspectra are easily identified as the two ^{195}Pt side bands.

The general behavior of the AB_2X system is illustrated in Figure 1. For simplicity of presentation and comparison with our observed spectra the parameters δ_{AB} = positive,

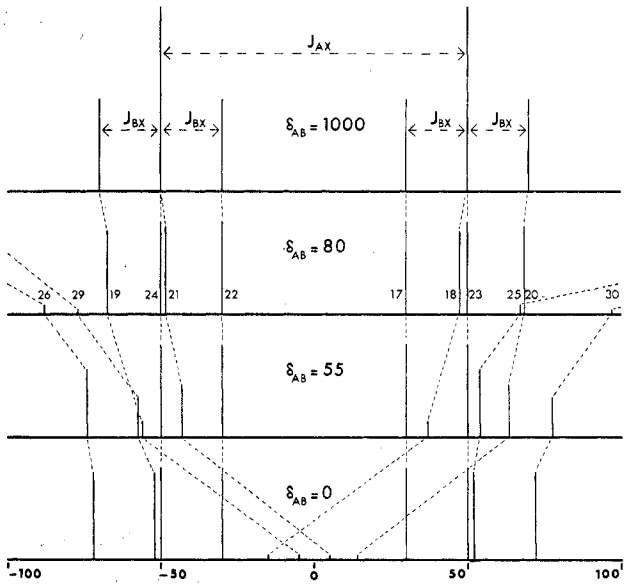

Figure 1. Line positions and intensities for the X region of the AB_2X spin system: $J_{AB} = -10$, $J_{AX} = +100$, $J_{BX} = -20$. Units are arbitrary provided all parameters are in the same units and line positions are given relative to the center of the multiplet (δ_X). The labeling of transitions (line numbers 17-26, 29, and 30; see δ_{AB} = 80 case) is from Table I and ref 3.

$J_{AB} = -10$ Hz, $J_{BX} = -20$ Hz, and $J_{AX} = +100$ Hz, have been used to produce this figure. Change of sign of δ_{AB} or J_{AB} causes inversion of the entire pattern and change of sign of both J_{AX} and J_{BX} has the same effect. If J_{AX} and J_{BX} have the same sign, then the outer lines of the triplets remain constant as δ_{AB} varies whereas in the case shown, having J_{AX} and J_{BX} of opposite sign, it is the inner lines which remain constant. First-order spectra are observed when $|J_{AB}| \ll ||\delta_{AB}| - {}^1/_2|J_{AX} - J_{BX}||$ and for a given J_{AB} the most complex spectra (*i.e.*, those having observable intensities[5] for all transitions) occur when $|\delta_{AB}| \simeq {}^1/_2||J_{AX} - J_{BX}| - |J_{AB}||$. This value of δ_{AB} is referred to below as δ_{AB}^{crit} and corresponds to δ_{AB} = 55 Hz in Figure 1. Figure 1 also shows that provided δ_{AB} is significantly above or below δ_{AB}^{crit} the spectrum may approximate to pairs of double doublets. This type of spectrum occurs for intermediate values of J_{AB} (*i.e.*, large enough to be non first order but not large enough to give appreciable intensity to other transitions) and the approximate criterion is ${}^1/_{20}||\delta_{AB}| - {}^1/_2|J_{AX} - J_{BX}|| < |J_{AB}| < {}^1/_5||\delta_{AB}| - {}^1/_2|J_{AX} - J_{BX}||$. However, the pattern is a perfectly symmetrical pair of double doublets only when $\delta_{AB} = 0$.

Returning to the platinum hydrides having mixed AB_2X-AB_2MX spectra, we note that, when J_{MX} is positive, δ_{AB}^{eff} for the low-field side band, center band, and high-field side band is given by $\delta_{AB} - {}^1/_2(J_{AM} - J_{BM})$, δ_{AB}, and $\delta_{AB} + {}^1/_2(J_{AM} - J_{BM})$, respectively.[6] Depending on the relative magnitudes of δ_{AB} and ${}^1/_2(J_{AM} - J_{BM})$, any of these may be in the non-first-order range. For example, if $\delta_{AB} \simeq \delta_{AB}^{crit}$ but ${}^1/_2|J_{AM} - J_{BM}| \gg \delta_{AB}$, then the center band is non first order and the side bands are first order, corresponding to the case observed by Roundhill for $[PtH(PPh_3)_3]^+$. Other combinations, such as a single non-first-order side band with the rest of the spectrum first order, are clearly possible.

(2) K. R. Dixon and J. J. McFarland, *J. Chem. Soc., Chem. Commun.*, 1274 (1972).

(3) R. J. Abraham, E. O. Bishop, and R. E. Richards, *Mol. Phys.*, 3, 485 (1960).

(4) J. A. Pople and P. Diehl, *Mol. Phys.*, 3, 545, 557 (1960); T. J. Batterham and R. Bramley, *Org. Magn. Resonance*, 3, 83 (1971).

(5) Except when J_{AB} is very large, since in this case a deceptively simple spectrum consisting of four equal-intensity doublets is observed. In the limit each doublet shows a splitting equal to J_{BX} and the pattern is symmetrical about δ_X.

(6) Low- and high-field side bands are reversed if J_{MX} is negative.

Table I. Transition Frequencies and Relative Intensities for the X Region of the AB_2X and AB_2MX Input Systems

	AB_2X[a]		AB_2MX	
No.[a]	Freq[b]	Rel intens	Freq[b]	Rel intens
17	$+^1/_2J_{AX} + J_{BX}$	1	$+^1/_2J_{AX} + J_{BX} + ^1/_2J_{MX}$	1
			$+^1/_2J_{AX} + J_{BX} - ^1/_2J_{MX}$	1
18	$+^1/_2J_{BX} + C^+\alpha - C^+\beta$	$\cos^2(\theta^+\alpha - \theta^+\beta)$	$+^1/_2J_{BX} + ^1/_2J_{MX} + C^+\alpha\alpha - C^+\beta\alpha$	$\cos^2(\theta^+\alpha\alpha - \theta^+\beta\alpha)$
			$+^1/_2J_{BX} - ^1/_2J_{MX} + C^+\alpha\beta - C^+\beta\beta$	$\cos^2(\theta^+\alpha\beta - \theta^+\beta\beta)$
19	$+^1/_2J_{BX} - C^+\alpha + C^+\beta$	$\cos^2(\theta^+\alpha - \theta^+\beta)$	$+^1/_2J_{BX} + ^1/_2J_{MX} - C^+\alpha\alpha + C^+\beta\alpha$	$\cos^2(\theta^+\alpha\alpha - \theta^+\beta\alpha)$
			$+^1/_2J_{BX} - ^1/_2J_{MX} - C^+\alpha\beta + C^+\beta\beta$	$\cos^2(\theta^+\alpha\beta - \theta^+\beta\beta)$
20	$-^1/_2J_{BX} + C^-\alpha - C^-\beta$	$\cos^2(\theta^-\alpha - \theta^-\beta)$	$-^1/_2J_{BX} + ^1/_2J_{MX} + C^-\alpha\alpha - C^-\beta\alpha$	$\cos^2(\theta^-\alpha\alpha - \theta^-\beta\alpha)$
			$-^1/_2J_{BX} - ^1/_2J_{MX} + C^-\alpha\beta - C^-\beta\beta$	$\cos^2(\theta^-\alpha\beta - \theta^-\beta\beta)$
21	$-^1/_2J_{BX} - C^-\alpha + C^-\beta$	$\cos^2(\theta^-\alpha - \theta^-\beta)$	$-^1/_2J_{BX} + ^1/_2J_{MX} - C^-\alpha\alpha + C^-\beta\alpha$	$\cos^2(\theta^-\alpha\alpha - \theta^-\beta\alpha)$
			$-^1/_2J_{BX} - ^1/_2J_{MX} - C^-\alpha\beta + C^-\beta\beta$	$\cos^2(\theta^-\alpha\beta - \theta^-\beta\beta)$
22	$-^1/_2J_{AX} - J_{BX}$	1	$-^1/_2J_{AX} - J_{BX} + ^1/_2J_{MX}$	1
			$-^1/_2J_{AX} - J_{BX} - ^1/_2J_{MX}$	1
23	$+^1/_2J_{AX}$	1	$+^1/_2J_{AX} + ^1/_2J_{MX}$	1
			$+^1/_2J_{AX} - ^1/_2J_{MX}$	1
24	$-^1/_2J_{AX}$	1	$-^1/_2J_{AX} + ^1/_2J_{MX}$	1
			$-^1/_2J_{AX} - ^1/_2J_{MX}$	1
25	$+^1/_2J_{BX} + C^+\alpha + C^+\beta$	$\sin^2(\theta^+\alpha - \theta^+\beta)$	$+^1/_2J_{BX} + ^1/_2J_{MX} + C^+\alpha\alpha + C^+\beta\alpha$	$\sin^2(\theta^+\alpha\alpha - \theta^+\beta\alpha)$
			$+^1/_2J_{BX} - ^1/_2J_{MX} + C^+\alpha\beta + C^+\beta\beta$	$\sin^2(\theta^+\alpha\beta - \theta^+\beta\beta)$
26	$+^1/_2J_{BX} - C^+\alpha - C^+\beta$	$\sin^2(\theta^+\alpha - \theta^+\beta)$	$+^1/_2J_{BX} + ^1/_2J_{MX} - C^+\alpha\alpha - C^+\beta\alpha$	$\sin^2(\theta^+\alpha\alpha - \theta^+\beta\alpha)$
			$+^1/_2J_{BX} - ^1/_2J_{MX} - C^+\alpha\beta - C^+\beta\beta$	$\sin^2(\theta^+\alpha\beta - \theta^+\beta\beta)$
29	$-^1/_2J_{BX} - C^-\alpha - C^-\beta$	$\sin^2(\theta^-\alpha - \theta^-\beta)$	$-^1/_2J_{BX} + ^1/_2J_{MX} - C^-\alpha\alpha - C^-\beta\alpha$	$\sin^2(\theta^-\alpha\alpha - \theta^-\beta\alpha)$
			$-^1/_2J_{BX} - ^1/_2J_{MX} - C^-\alpha\beta - C^-\beta\beta$	$\sin^2(\theta^-\alpha\beta - \theta^-\beta\beta)$
30	$-^1/_2J_{BX} + C^-\alpha + C^-\beta$	$\sin^2(\theta^-\alpha - \theta^-\beta)$	$-^1/_2J_{BX} + ^1/_2J_{MX} + C^-\alpha\alpha + C^-\beta\alpha$	$\sin^2(\theta^-\alpha\alpha - \theta^-\beta\alpha)$
			$-^1/_2J_{BX} - ^1/_2J_{MX} + C^-\alpha\beta + C^-\beta\beta$	$\sin^2(\theta^-\alpha\beta - \theta^-\beta\beta)$

[a] Transition numbers are those used for the AB_2X system in ref 3. Equations for the AB_2X system are from this reference except for a change in notation to bring it in line with the more systematic and general treatments of this type of system given in ref 4. [b] Transition frequencies are relative to the chemical shift of X (*i.e.*, δ_X should be added to each expression). The C and θ values are defined by the following expressions where C can be positive or negative and $-\pi/4 < \theta < \pi/4$ (see ref 4): $C^+\alpha \cos 2\theta^+\alpha = {}^1/_2\delta_{AB} + {}^1/_4J_{AB} + {}^1/_4(J_{AX} - J_{BX})$, $C^+\beta \cos 2\theta^+\beta = {}^1/_2\delta_{AB} + {}^1/_4J_{AB} - {}^1/_4(J_{AX} - J_{BX})$, $C^-\alpha \cos 2\theta^-\alpha = {}^1/_2\delta_{AB} - {}^1/_4J_{AB} + {}^1/_4(J_{AX} - J_{BX})$, $C^-\beta \cos 2\theta^-\beta = {}^1/_2\delta_{AB} - {}^1/_4J_{AB} - {}^1/_4(J_{AX} - J_{BX})$, $C^+\alpha\alpha \cos 2\theta^-\alpha\alpha = {}^1/_2\delta_{AB} + {}^1/_4J_{AB} + {}^1/_4(J_{AX} - J_{BX}) + {}^1/_4(J_{AM} - J_{BM})$, $C^+\alpha\beta \cos 2\theta^+\alpha\beta = {}^1/_2\delta_{AB} + {}^1/_4J_{AB} + {}^1/_4(J_{AX} - J_{BX}) - {}^1/_4(J_{AM} - J_{BM})$, $C^+\beta\alpha \cos 2\theta^+\beta\alpha = {}^1/_2\delta_{AB} + {}^1/_4J_{AB} - {}^1/_4(J_{AX} - J_{BX}) + {}^1/_4(J_{AM} - J_{BM})$, $C^+\beta\beta \cos 2\theta^+\beta\beta = {}^1/_2\delta_{AB} + {}^1/_4J_{AB} - {}^1/_4(J_{AX} - J_{BX}) - {}^1/_4(J_{AM} - J_{BM})$, $C^-\alpha\alpha \cos 2\theta^-\alpha\alpha = {}^1/_2\delta_{AB} - {}^1/_4J_{AB} + {}^1/_4(J_{AX} - J_{BX}) + {}^1/_4(J_{AM} - J_{BM})$, $C^-\alpha\beta \cos 2\theta^-\alpha\beta = {}^1/_2\delta_{AB} - {}^1/_4J_{AB} + {}^1/_4(J_{AX} - J_{BX}) - {}^1/_4(J_{AM} - J_{BM})$, $C^-\beta\alpha \cos 2\theta^-\beta\alpha = {}^1/_2\delta_{AB} - {}^1/_4J_{AB} - {}^1/_4(J_{AX} - J_{BX}) + {}^1/_4(J_{AM} - J_{BM})$, $C^-\beta\beta \cos 2\theta^-\beta\beta = {}^1/_2\delta_{AB} - {}^1/_4J_{AB} - {}^1/_4(J_{AX} - J_{BX}) - {}^1/_4(J_{AM} - J_{BM})$, and $C \sin 2\theta = 2^{-1/2} J_{AB}$ for all C's and θ's.

$[PtH(PEt_3)_3]^+$. The hydride resonance for this complex at 60 MHz consists of a complex center band (see Figure 2A) and an upfield ^{195}Pt side band showing a first-order doublet of triplets (see Figure 1). The low-field side band is partially obscured by ethyl proton resonances. At 220 MHz the low-field side band and the center band are both first order but the high-field side band is more complex (see Figure 2B). No differences are detected between ClO_4^- and BPh_4^- salts and low-temperature (−40°) spectra give no evidence for phosphine-exchange processes. Proton-decoupled ^{31}P spectra at 40.5 MHz are typical of an AB_2 system with the A resonance appearing as a broad unresolved absorption and the B resonance as a slightly asymmetric doublet. The expected ^{195}Pt side bands are observed; an interesting point being that the low-field B side band appears as a doublet but the high-field side band is not resolved. This may be another example of the effective chemical shift phenomenon discussed above but it may also be caused by incomplete proton decoupling in those molecules containing ^{195}Pt. ^{31}P spectra were also recorded at 19.3 MHz without proton decoupling giving similar results except that splitting of the A resonance by the X proton was observed.

Measurement of these spectra gives the parameters shown in Table II. Most of these are derived from direct measurement of peak separations[7] and the indicated errors are estimates of the accuracy of location of band centers. However, in the ^{31}P spectra the broad peaks coupled with signal to noise problems made accurate measurement difficult and consequently δ_{AB}, J_{AM}, and J_{BM} are mean values from measurements of seven independent spectra and the indicated errors are standard deviations. The signs of the various parameters are discussed below.

Table II. Observed Coupling Constants (Hz) and Chemical Shifts (ppm)[a]

	$[PtH(PEt_3)_3]^+$	*trans*-$[PtH(PEt_3)_2(PPh_3)]^+$	$[PtH(PPh_3)_3]^+$
J_{AB}	−17.5 ± 0.5	−18.0 ± 1.0	±18.2 ± 0.2[b]
J_{AX}	+158.5 ± 0.5	+166.5 ± 0.5	+160.0 ± 0.5
J_{BX}	−16.25 ± 0.25	−14.75 ± 0.25	−12.5 ± 0.25
J_{AM}	+2037 ± 19	+2094 ± 20[b]	[c]
J_{BM}	+2515 ± 21	+2480 ± 20	[c]
J_{MX}	+791 ± 1	+894 ± 1	+775 ± 1
δ_{AB}[d]	+3.31 ± 0.2	−3.60 ± 0.2	<0.6[b]
δ_B	−17	−16.5	+3
δ_X	+6.25	+6.35	+5.74

[a] From TMS or H_3PO_4; positive values denote upfield shifts. [b] Calculated from spectral fitting; other values are directly measured from spectra except for a small correction for non-first-order distortion in δ_{AB}. [c] Not observed. [d] Positive values denote A upfield of B.

At a magnetic flux density of 1.4092 T (*i.e.*, ^1H at 60 MHz), $\delta_{AB} = 80$ Hz and $\delta_{AB}^{crit} = 78.6$ Hz, and the center-band hydride resonance therefore lies in the most complex spectral range (see Figure 1). It might be expected that analysis as an AB_2X system would correctly predict the appearance of this center-band spectrum with the ethyl protons contributing only a general line-broadening effect but unfortunately this is not the case. Not only are the trans phosphorus atoms magnetically nonequivalent (which has little effect provided $^2J_{PP}$ is large) but the ethyl protons also play a significant role when δ_{AB} is close to δ_{AB}^{crit}. The effect may be understood by regarding an ethyl proton as the M of an AB_2MX system with $J_{MX} = 0$. The subspectra having $\delta_{AB}^{eff} = \delta_{AB} \pm {}^1/_2(J_{AM} - J_{BM})$

(7) A small correction for the non-first-order distortion is necessary in evaluating δ_{AB}.

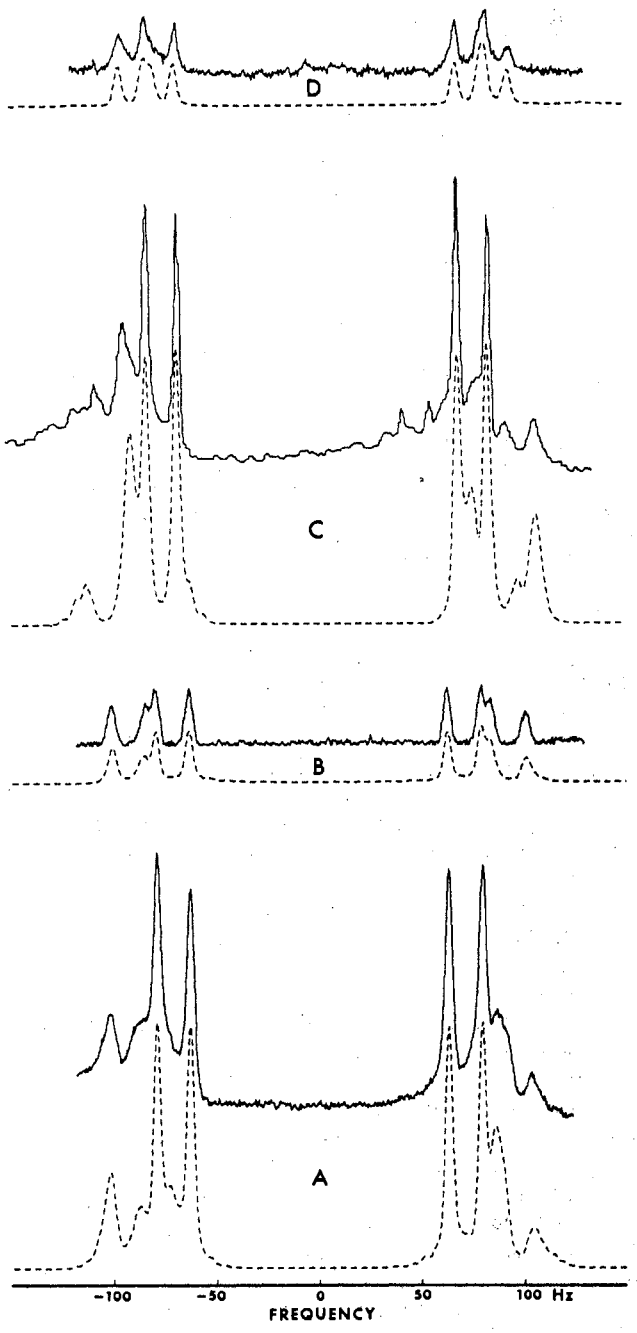

Figure 2. Observed (solid lines) and calculated (dashed lines) spectra: only the non-first-order sections of the hydridic hydrogen resonances are shown. The frequency scale is in hertz relative to the centers of the multiplets: A, center band for $[PtH(PEt_3)_3]^+$ at 60 MHz; B, high-field ^{195}Pt side band for $[PtH(PEt_3)_3]^+$ at 220 MHz; C, center band for *trans*-$[PtH(PEt_3)_2(PPh_3)]^+$ at 60 MHz; D, low-field ^{195}Pt side band for *trans*-$[PtH(PEt_3)_2(PPh_3)]^+$ at 220 MHz.

are then superimposed. If M is a methyl proton, then $^1/_2(J_{AM} - J_{BM}) \simeq 8$ Hz and the subspectra are very similar to each other unless δ_{AB} is close to δ_{AB}^{crit}. However, in the critical region the subspectra differ in both line positions and intensity and superposition of the subspectra does not lead to a simple broadening of the AB_2X spectrum but significant shifts in peak maxima and intensities are introduced. The effect is most marked for the outermost lines (no. 26 and 30 in Figure 1), which are the most sensitive to δ_{AB}, and calculations using the AB_2X model always predict more asymmetric positions (with respect to the center of the multiplet) than are observed for these lines.

Clearly, one proton cannot adequately describe the effect of the 45 ethyl protons! Moreover the system has 49 magnetically active nuclei and is far too complex for computer simulation[8] but various approximations were tried, with the following model proving the most successful

$$(H_Y)_3C-C(H_Z)_2-P_A-\overset{\overset{P_B}{|}}{Pt}-H_X \quad \underset{|}{P_{B'}}$$

The dashed line in Figure 2A shows the 60-MHz center-band spectrum computed using this model with the chemical shifts and coupling constants shown in Table II together with typical values for other parameters ($J_{BB'} = +90$ Hz, $J_{YZ} = +7.5$ Hz, $J_{AY} = +16.0$ Hz, $J_{AZ} = -7.0$ Hz, $\delta_Y = -0.96$ ppm, $\delta_Z = -1.73$ ppm). δ_Y and δ_Z are observed values but the intraligand couplings are taken from the literature report[9] for *trans*-$[PtCl_2(PEt_3)_2]$ because the ethyl region of the $[PtH(PEt_3)]^+$ spectrum was too badly overlapped to allow determination of these parameters. All long-range couplings (*i.e.*, $J_{BY}, J_{BZ}, J_{XY}, J_{XZ}$, etc.) were assumed to be zero.

Considering the magnitude of the approximation, the agreement with the observed spectrum is excellent. Various other approximations (for example, one can place one methyl or one methylene proton on each phosphorus) give similar simulated spectra but the position of the outer lines is sensitive to the nature of the approximation. Consequently, although it is possible to improve the fit shown in Figure 2A by adjustment of δ_{AB} and J_{AB}, we do not consider this refinement to be justified.

The parameters shown in Table II give a value of 56 Hz for δ_{AB}^{eff} ($=\delta_{AB} + {}^1/_2(J_{AM} - J_{BM})$) for the high-field side band at a magnetic flux density of 5.167 T (*i.e.*, ^1H at 220 MHz). Use of this value in the approximation shown above gives the dashed spectrum in Figure 2B. The agreement is again excellent and in this case the calculated spectrum is not very dependent on the approximation used since δ_{AB}^{eff} is fairly far from δ_{AB}^{crit} (78.6 Hz). Calculations using an AB_2X analysis for the low-field side band and center band at 220 MHz and high-field side band at 60 MHz ($\delta_{AB}^{eff} = +534$, +295 and −159 Hz, respectively) confirm our analysis by correctly predicting the observed first-order patterns.[10] Simulation of the ^{31}P spectrum also gives excellent agreement.

Finally, we note that the 100-MHz spectrum of $[PtH(PEt_3)_3][ClO_4]$ has been reported previously.[11] Simulation of the spectrum using our parameters gives a slightly distorted doublet of triplets with apparent coupling constants $J_{AX} = 156.1$ Hz and $J_{BX} = 15.0$ Hz in excellent agreement with the reported values of 156.0 and 15.0 Hz.

trans-$[PtH(PEt_3)_2(PPh_3)]^+$. Spectra of this cation were recorded with the ClO_4^- salt and are basically similar to those described for $[PtH(PEt_3)_3]^+$ except that it is now the low-field side band at 220 MHz which is non first order in the ^1H spectrum and the low-field side band which is not resolved in the ^{31}P spectrum. These reversals are expected since δ_{AB} is negative for *trans*-$[PtH(PEt_3)_2(PPh_3)]^+$ and positive for $[PtH(PEt_3)_3]^+$. The measured parameters for *trans*-$[PtH(PEt_3)_2(PPh_3)]^+$ are given in Table II with errors estimated from accuracy of location of band centers and the non-first-order sections of the hydride resonances are shown in Figures 2C and 2D. The A resonances in ^{31}P spectra were too weak

(8) The UEAITR program used here has a limit of 7 nuclei having a maximum product of multiplicities of 216.

(9) W. McFarlane, *J. Chem. Soc. A*, 1922 (1967).

(10) δ_{AB}^{eff} values calculated from δ_{AB}, J_{AM}, and J_{BM} in Table II. The 60-MHz side band shows some distortion from first order.

(11) M. J. Church and M. J. Mays, *J. Chem. Soc. A*, 3074 (1968).

to permit observation of ^{195}Pt side bands and the value of J_{AM} is therefore calculated from fitting of the low-field ^1H side band at 220 MHz.

Problems with the simulation of spectra are similar to those described above and are complicated by the fact that intraligand coupling constants are not well known for coordinated phenylphosphine ligands. Moreover, 220-MHz ^1H spectra show the presence of hydridic impurities (*ca.* 10%, possibly *cis*-$[PtH(PEt_3)_2(PPh_3)]^+$ and other $[PtH(PEt_3)_n(PPh_3)_{3-n}]^+$ species) which are not removed by recrystallization procedures. Consequently, some of the weaker bands in the 60-MHz ^1H spectrum (Figure 2C) may be due to these impurities. Approximate simulations of the observed spectra were tried with a model having three protons in one of the phenyl groups and also with the model

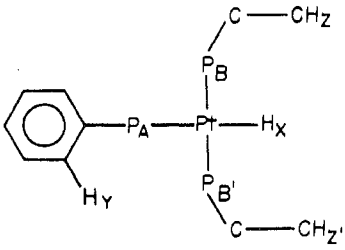

Results for this model are shown as the dashed lines in Figures 2C and 2D. The parameters used were those given in Table II together with $J_{AY} = +7.1$ Hz, $\delta_Y = -7.70$ ppm, and $\delta_Z = -1.00$ ppm. The chemical shifts were observed, J_{AY} is the literature value for free triphenylphosphine,[12] and the other couplings were similar to those used above for $[PtH(PEt_3)_3]^+$. Considering the approximation and impurity problems the agreement is good at 60 MHz and excellent at 220 MHz. The spectrum at 60 MHz is very sensitive to the approximation used and further refinement is not justified but the value of δ_{AB}^{eff} (−128 Hz) for the low-field side band at 220 MHz is a "best fit" value which was subsequently used to calculate J_{AM}. $\delta_{AB}^{eff} = -128$ Hz is sufficiently far removed from $\delta_{AB}^{crit} = 81.6$ Hz that the nature of the approximation is not important and in fact an AB_2X analysis can be used if desired. The AB_2X analysis also correctly predicts the observed first-order spectra for the high-field side band and center band at 220 MHz and the high-field side band at 60 MHz ($\delta_{AB}^{eff} = -513$, −321, and −281 Hz, respectively).[13]

Simulation of the 100-MHz spectrum of *trans*-$[PtH(PEt_3)_2(PPh_3)]^+$ gives an almost first-order spectrum with apparent coupling constants $J_{AX} = 164.4$ Hz and $J_{BX} = 13.7$ Hz which is again good agreement with the literature report[11] of 165 and 14.4 Hz.

$[PtH(PPh_3)_3]^+$. Spectra of this cation recorded at 60 MHz for both BF_4^- and $(CF_3COO)_2H^-$ salts were very similar to the 100-MHz spectrum reported by Roundhill and coworkers[1] for the $(CF_3COO)_2H^-$ salt (see Figure 2 in ref 1). The center band resonance is of the pair of double doublets type discussed above and its symmetry shows that δ_{AB} is very small (<15 Hz at 1.4092 T, assuming that our line positions at 60 MHz are accurate ±0.1 Hz). Models involving the phenyl protons are unnecessary since δ_{AB}^{crit} (77.2 Hz) is well removed from δ_{AB} and analysis as an AB_2X system using the parameters from Table II gives the results shown in Table III. Agreement with our observed line positions at 60 MHz and with those of Roundhill at 100 MHz is excellent and in both cases the side bands are predicted to be first order provided

(12) R. Keat, *Chem. Ind. (London)*, 46, 1362 (1968).
(13) Values calculated from δ_{AB}, J_{AM}, and J_{BM} in Table II.

Table III. Observed and Calculated Spectra for $[PtH(PPh_3)_3]^+$ [a]

Line no.[b]	Calcd[c] Freq, Hz	Calcd[c] Intens[e]	Obsd freq, Hz[d] 60 MHz	Obsd freq, Hz[d] 100 MHz[f]
17	+67.5	1.00	+67.5	+67
18	+2.5	0.08	*g*	*g*
19	−15.0	0.08	*g*	*g*
20	−2.5	0.08	*g*	*g*
21	+15.0	0.08	*g*	*g*
22	−67.5	1.0	−67.5	−67
23	+80.0	1.0	+79.9	+80
24	−80.0	1.0	−80.1	−80
25	+83.8	0.92	+83.8	+84
26	−96.3	0.92	−96.3	−97
29	−83.8	0.92	−83.8	−84
30	+96.3	0.92	+96.3	+97

[a] Only the center-band portion of the hydride resonance is shown. [b] Numbering of transitions is from ref 3. [c] $J_{AX} = 160$ Hz, $J_{BX} = -12.5$ Hz, $\delta_{AB} = 0$. Spectrum is independent of observation frequency if $\delta_{AB} = 0$. [d] Frequencies are in Hz relative to the center of the multiplet and are accurate to ±0.1 Hz for the 60-MHz spectrum. The precision of the 100-MHz data is not known. [e] Observed lines were all of approximately equal intensity. [f] Data from ref 1. [g] Not observed.

$\frac{1}{2}(J_{AM} - J_{BM}) > 250$ Hz (assuming resolution of 0.5 Hz). Roundhill and coworkers did not report δ_{AB}, J_{AM}, or J_{BM} and our ^{31}P spectra were not of sufficient quality to enable us to determine these values but the requirements that $\delta_{AB} <$ 0.6 ppm and $\frac{1}{2}(J_{AM} - J_{BM}) > 250$ Hz are entirely consistent with our observed values for the other complexes. The values of J_{AX}, J_{BX}, and J_{MX} given in Table III for $[PtH(PPh_3)_3]^+$ are directly measured from the spectra, and errors are estimates from accuracy of location of band centers and the value and error limits for J_{AB} are derived from the analysis of the X spectrum (Table III) assuming that peak positions are accurate ±0.1 Hz.

Signs of Coupling Constants. The observed spectra for $[PtH(PEt_3)_3]^+$ give the relative signs of J_{AX}, J_{BX}, and J_{AB} and also those for J_{AM}, J_{BM}, and J_{MX} but the two groups cannot be interrelated in the absence of further information. However, the absolute signs of the coupling constants in *trans*-$[PtHCl(PEt_3)_2]$ have been determined previously[14] ($^1J_{Pt-H}$ positive and $^2J_{P-H}$ negative) and it is reasonable to assume that the corresponding couplings in our complexes have the same signs (*i.e.*, J_{MX} positive and J_{BX} negative). With these assumptions the set of signs shown in Table II is derived as follows. Inspection of Table I and Figure 1 shows that lines 17 and 22 remain constant as δ_{AB} varies and are separated by $J_{AX} + 2J_{BX}$. The observed magnitude of this separation in the center band at 60 MHz (Figure 2A) is 126 Hz, and consequently if J_{BX} is negative (16.25 Hz), then J_{AX} is positive (158.5 Hz). Furthermore, the direction of the asymmetry shown in Figure 2A shows that J_{AB} is negative. If J_{MX} is positive, then the high-field ^{195}Pt side bands have $\delta_{AB}^{eff} = \delta_{AB} + \frac{1}{2}(J_{AM} - J_{BM})$. At a magnetic flux density of 5.167 T (*i.e.*, ^1H at 220 MHz), $\delta_{AB} = +295$ Hz and δ_{AB}^{eff} has an observed magnitude of 56 Hz and must in fact be positive since the observed magnitudes of $\frac{1}{2}J_{AM}$ and $\frac{1}{2}J_{BM}$ cannot be combined with δ_{AB} so as to produce a value of −56 Hz. It follows that $+\frac{1}{2}(J_{AM} - J_{BM}) = -239$ Hz, and from the observed magnitudes of J_{AM} and J_{BM} this can only be true if both are positive. This is in agreement with previous determinations[9] of the sign of $^1J_{Pt-P}$ in square-planar complexes. Our results appear to be the first sign determinations of P–P coupling constants and of $^2J_{P-H}$ (trans) in platinum(II) complexes, the only comparable measurements being the reported

(14) W. McFarlane, *Chem. Commun.*, 772 (1967).

positive values of $^2J_{P-P}$ in *cis*-$[PdCl_2(P(OMe)_3)_2]$ and *trans*-$[PdI_2(PMe_3)_2]$. However our results are in agreement with general ideas that large trans couplings are positive while the smaller cis couplings can have either sign.[15]

A similar line of reasoning gives the signs shown in Table II for the couplings in the *trans*-$[PtH(PEt_3)_2(PPh_3)]^+$ cation. However, the symmetry of the $[PtH(PPh_3)_3]^+$ spectra precludes the determination of any sign information except that J_{AX} and J_{BX} must be of opposite sign.

Conclusions

The above discussion clearly shows that the unusual spectra reported by Roundhill and coworkers[1] for $[PtH(PPh_3)_3]$-$[(CF_3COO)_2H]$ can be completely interpreted on the basis of an ionic structure having a square-planar cation. Thus, the previous workers were correct in suggesting that non-first-order effects offer a better explanation of the spectra than does the postulate of chemical nonequivalence of the B phosphorus atoms caused by ion association. More generally our results show that different side- and center-band multiplets are expected to be common for any A_nB_mX or similar spin system. These become A_nB_mMX systems in molecules containing ^{195}Pt and the side- and center-band patterns are similar only when $|\delta_{AB}| \gg {}^1/_2|J_{AM} - J_{BM}|$. An example of an AB system showing these effects was recently observed by us in the ^{31}P spectrum of the $[PtCl(o\text{-phen})(PEt_3)_2]^+$ cation which has chemically nonequivalent triethylphosphine groups. The spectrum consists of a poorly resolved central doublet (AB system) with the ^{195}Pt side bands having a quartet structure (ABM system).[16]

Our analysis also demonstrates that when δ_{AB} is close to certain critical values,[17] it is not possible to neglect the effect on the X spectrum of remote magnetically active nuclei which are coupled to A or B. Thus in tertiary phosphine complexes it may not be possible to neglect the effects of remote hydrogens in the alkyl or aryl groups.

Experimental Section

The complexes $[PtH(PEt_3)_3][BPh_4]$,[18] $[PtH(PEt_3)_3][ClO_4]$,[11] *trans*-$[PtH(PEt_3)_2(PPh_3)][ClO_4]$,[11] $[PtH(PPh_3)_3][(CF_3COO)_2H]$,[1] and $[PtH(PPh_3)_3][BF_4]$[19] were prepared as previously described. Nuclear magnetic resonance spectra were recorded in dichloromethane solution using tetramethylsilane as internal reference for proton spectra and phosphoric acid as external reference for phosphorus spectra. Chemical shifts are reported in Hz or ppm as appropriate and positive values indicate resonances to high field of the reference. Proton spectra were recorded at 60 MHz on a Varian HA60 spectrometer and at 220 MHz by the Canadian 220 MHz NMR Centre, Sheridan Park, Ontario. Phosphorus spectra were recorded at 19.3 MHz on a Varian HA60 spectrometer and at 40.5 MHz on a Varian XL100 spectrometer. Simulated spectra were calculated using the UEAITR program[20] on an IBM 370/145 computer and plotted on a Calcomp 563 Drum Plotter using a program based on the NMR PLOT program.[21]

Acknowledgments. We thank the National Research Council of Canada and the University of Victoria for research grants and Dr. E. J. Wells for the use of the Varian XL100 spectrometer at Simon Fraser University.

Registry No. $[PtH(PEt_3)_3]^+$, 48074-87-9; *trans*-$[PtH(PEt_3)_2(PPh_3)]^+$, 47757-13-1; $[PtH(PPh_3)_3]^+$, 47899-53-6; P, 7723-14-0; ^{195}Pt, 14191-88-9.

(15) E. G. Finer and R. K. Harris, *Progr. Nucl. Magn. Resonance Spectrosc.*, 6, 61 (1971), and references therein.

(16) $J_{AB} = 22$ Hz, $J_{AM} = 3680$ Hz, $J_{BM} = 3490$ Hz, and $\delta_{AB} = 14$ Hz at 40.5 MHz.

(17) ${}^1/_2|J_{AX} - J_{BX}| - |J_{AB}|$ in the particular case of the AB_2X system studied here.

(18) H. C. Clark and K. R. Dixon, *J. Amer. Chem. Soc.*, 91, 596 (1969).

(19) F. Cariati, R. Ugo, and F. Bonati, *Inorg. Chem.*, 5, 1128 (1966).

(20) R. B. Johannesen, J. A. Ferretti, and R. K. Harris, *J. Magn. Resonance*, 3, 84 (1970).

(21) J. D. Swalen in "Computer Programs for Chemistry," Vol I, D. F. Detar, Ed., W. A. Benjamin, New York, N. Y., 1968.

Contribution from the Department of Chemistry, University of Rajasthan, Jaipur-302004, India

Kinetics and Mechanism of the Electron-Transfer Reactions of Aquo- and Coordinated Thallium(III). VII. Reduction of Chlorothallium(III) Complexes by Hypophosphite

K. S. GUPTA* and Y. K. GUPTA

Received March 21, 1973

The Tl^{III}–H_3PO_2 reaction is catalyzed by chloride ions. The rate first decreases, reaches a minimum at $[Cl^-]_T/[Tl^{III}]_T \simeq 1$, and then increases to a limiting value when this ratio is *ca.* 50. The reactivity of various thallium(III) species follows the order $TlCl_4^- > TlCl_3 > TlCl_2^+ > Tl^{3+} > TlCl^{2+}$. The reactive hypophosphite species is H_3PO_2. The complicated rate law for the reaction is

$$-d[Tl^{III}]/dt = (kK[Tl^{3+}] + k_1[TlCl^{2+}] + k_2[TlCl_2^+] + k_3[TlCl_3] + k_4[TlCl_4^-])\{[H_3PO_2]_T[H^+]/([H^+] + K_d)\}$$

where K_d is the dissociation constant of H_3PO_2, k, k_1, k_2, k_3, and k_4 are the rate constants for the various reactive species of Tl^{III}, and K is the formation constant for the complex of Tl^{3+} and H_3PO_2.

Introduction

A kinetics study of the oxidation of hypophosphite[1,2] has recently been made and the following mechanism was suggested

$$Tl^{3+} + H_3PO_2 \overset{K}{\rightleftharpoons} TlH_3PO_2^{3+} \quad (1)$$

$$TlH_3PO_2^{3+} + H_2O \overset{k}{\rightarrow} Tl^+ + H_3PO_3 + 2H^+ \quad (2)$$

The rate law is

$$\frac{-d[Tl^{III}]}{dt} = \frac{kK[Tl^{III}][H_3PO_2]}{1 + K[H_3PO_2]} \quad (3)$$

(1) K. S. Gupta and Y. K. Gupta, *J. Chem. Soc. A*, 256 (1970).

(2) K. S. Gupta and Y. K. Gupta, *Indian J. Chem.*, 8, 1001 (1970).